Cell

A Combinatorial Code for CPE-Mediated Translational Control

Maria Piqué,[1] José Manuel López,[1,2] Sylvain Foissac,[1] Roderic Guigó,[1] and Raúl Méndez[1,*]
[1]Centre for Genomic Regulation (CRG), UPF, C/Dr. Aiguader, 88, 08003 Barcelona, Spain
[2]Present address: Instituto de Neurociencias, Edificio M, Campus de Bellaterra, Universidad Autónoma de Barcelona, 08193 Cerdanyola del Vallès, Barcelona, Spain.
*Correspondence: raul.mendez@crg.es
DOI 10.1016/j.cell.2007.12.038

SUMMARY

Cytoplasmic polyadenylation plays a key role in the translational control of mRNAs driving biological processes such as gametogenesis, cell-cycle progression, and synaptic plasticity. What determines the distinct time of polyadenylation and extent of translational control of a given mRNA, however, is poorly understood. The polyadenylation-regulated translation is controlled by the cytoplasmic polyadenylation element (CPE) and its binding protein, CPEB, which can assemble both translational repression or activation complexes. Using a combination of mutagenesis and experimental validation of genome-wide computational predictions, we show that the number and relative position of two elements, the CPE and the Pumilio-binding element, with respect to the polyadenylation signal define a combinatorial code that determines whether an mRNA will be translationally repressed by CPEB, as well as the extent and time of cytoplasmic polyadenylation-dependent translational activation.

INTRODUCTION

The mechanism of cytoplasmic polyadenylation, which controls the translation of many key mRNAs in vertebrates, has been elucidated in meiotic maturation of *Xenopus* oocytes. Meiotic progression requires the translational activation of specific stored maternal mRNAs at different steps of the cell cycle. The extent of translational activation of these maternal mRNAs is also finely regulated resulting in differential rates of product accumulation that, combined with the control of protein degradation, establish phase-specific peaks of expression of the factors that drive meiotic progression. The most extensively studied mechanism to maintain repressed maternal mRNAs in arrested oocytes and to activate translation during meiotic resumption is mediated by the cytoplasmic polyadenylation element binding protein (CPEB) (for reviews see Mendez and Richter, 2001; Richter, 2007). Cytoplasmic polyadenylation requires two elements in the 3′UTRs of responding mRNAs, the hexanucleotide AAUAAA (Hex) (Sheets et al., 1994), which is bound by the cleavage and polyadenylation specificity factor (CPSF) (Bilger et al., 1994; Dickson et al., 1999) and the nearby cytoplasmic polyadenylation element (CPE), which recruits CPEB (Fox et al., 1989; Hake and Richter, 1994). CPEB also mediates translational repression (masking) of maternal mRNAs in unstimulated oocytes by recruiting Maskin (Stebbins-Boaz et al., 1999). Another *trans*-acting factor recruited by some repressed CPE-containing 3′UTRs is *Xenopus* Pumilio (Pum), an RNA-binding protein that interacts with CPEB (Nakahata et al., 2001; Nakahata et al., 2003).

However, individual CPE-containing mRNAs display specific translational behavior during meiosis, suggesting that individual features within their 3′UTRs determine their response to CPEB-mediated translational control. Thus, not every CPE-containing mRNA is masked (Barkoff et al., 2000; de Moor and Richter, 1999) and not every CPE-containing mRNA is polyadenylated at the same time. While some mRNAs, such as the one encoding Mos, are polyadenylated "early" at prophase I, other mRNAs, such that encoding cyclin B1, are polyadenylated "late" at metaphase I (MI). These events establish a hierarchical translational activation during meiotic progression. "Early" polyadenylation is directly triggered by the Aurora A-mediated phosphorylation of CPEB (Mendez et al., 2000a), which increases its affinity for CPSF and the cytoplasmic poly(A) polymerase GLD-2 (Barnard et al., 2004; Mendez et al., 2000b; Rouhana et al., 2005), and decreases its affinity for PARN, a poly(A)-specific ribonuclease (Kim and Richter, 2006). "Late" polyadenylation requires Mos synthesis and phosphorylation of CPEB by Cdc2 kinase, which targets most of the CPEB for destruction (Ballantyne et al., 1997; de Moor and Richter, 1997; Reverte et al., 2001; Mendez et al., 2002).

Despite the knowledge accumulated on the composition and regulation of the protein complexes that mediate translational repression and activation of CPE-containing mRNAs, the 3′UTR features that define whether an mRNA is a target for CPEB-mediated translational repression and how the time and extent of cytoplasmic polyadenylation-dependent translational activation is controlled are still unclear. In the last years, a number of different hypothesis have been postulated. Thus, translational repression by CPEB has been suggested to be determined by specific sequences overlapping with the CPE, by the number of CPEs in an additive dose-dependent manner or additional

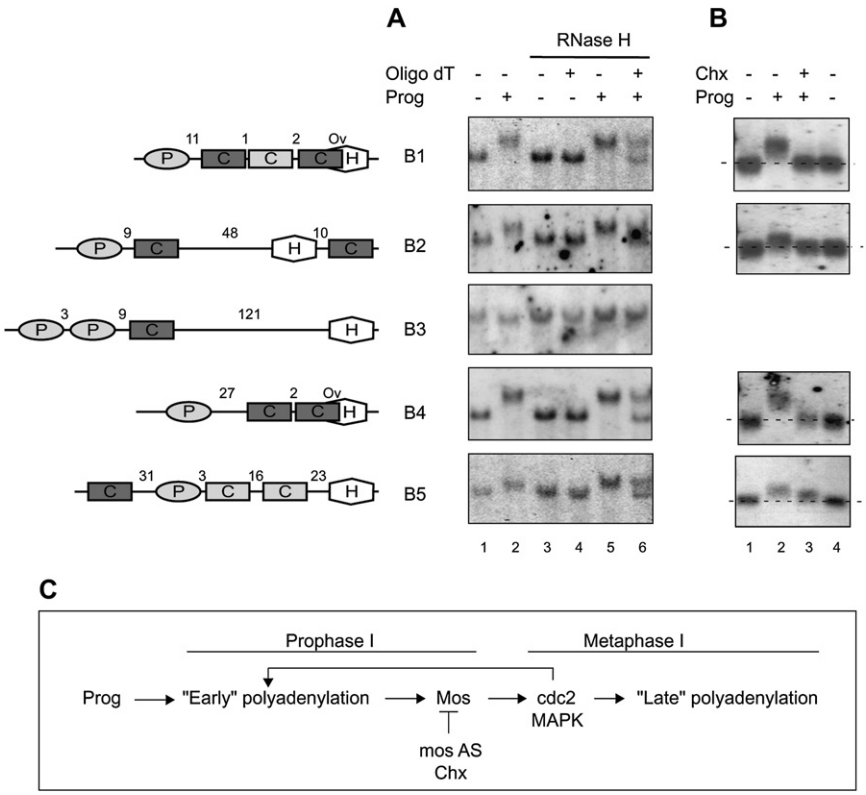

Figure 1. Cytoplasmatic Polyadenylation of Endogenous Cyclin B1–B5 mRNAs during *Xenopus* Oocyte Maturation

(A) Stage VI oocytes were treated with or without Prog and collected 1 hr after maturation. Total RNA was extracted and analyzed by northern blot with cyclin B1–B5 DNA probes. The extent of polyadenylation was measured by treatment with oligo (dT) and RNase H.

(B) Requirement of Cdc2 activation for polyadenylation was determined by treating the oocytes with or without Chx and Prog. All oocytes were collected 2 hr after maturation of the control oocytes. Total RNA was extracted and analyzed by northern blot. Schematic representation of the 3′UTRs of *Xenopus* cyclins B1–B5 is shown on the left. Putative CPEs (C, either consensus as dark gray boxes or nonconsensus as light gray boxes), PBEs (P, as gray ovals), and Hexs (H, as open hexagons) elements and the distances between them, in nts, are indicated. "Ov" refers to an overlapping CPE with Hex.

(C) Schematic representation of the sequential cytoplasmic polyadenylations. The positive feedback loop from cdc2 activation to the "early" polyadenylation and effect of Mos AS and Chx are indicated.

cis-acting elements, such as the Pumilio-binding element (PBE) (Barkoff et al., 2000; de Moor and Richter, 1999; Nakahata et al., 2003). The temporally different patterns of polyadenylation of CPE-containing mRNAs have been attributed to a number of 3′UTR features, including the CPE sequence, elements adjacent to the CPE, the position or number of CPEs (Ballantyne et al., 1997; de Moor and Richter, 1997; Mendez et al., 2002), additional *cis*-acting elements, such as PBE (Nakahata et al., 2003), or even a CPE/CPEB-independent "early" polyadenylation mediated by the translational repressor Musashi (Okano et al., 2002; Charlesworth et al., 2006). Finally, very little is known about how the extent of polyadenylation of each individual mRNA is controlled.

In this manuscript we focus on the translational regulation and cytoplasmic polyadenylation driven by the 3′UTRs of *Xenopus* cyclin B1–B5 mRNAs as a model system to dissect the role of the *cis*-acting elements present in their 3′UTRs in the qualitative and quantitative CPEB-dependent regulation of translational repression and activation. The comparative analysis of these 3′UTRs allow us to define a combinatorial code where the number and relative position of three elements, the CPE, the PBE, and the Hex, determine whether an mRNA is going to be translationally repressed by CPEB, as well as the extent and time of cytoplasmic polyadenylation-dependent translational activation. We translate these combinations of motifs into algorithms to identify vertebrate mRNAs potentially regulated by CPEB. The accuracy of the predictions is tested by experimental analysis of the translational control driven by a random selection of the newly identified CPE-containing 3′UTRs.

RESULTS

Cytoplasmic Polyadenylation of Cyclin B1–B5 mRNAs in Response to Progesterone

To determine if there is a correlation between the *cis*-acting elements present in a 3′UTR and the extent and timing of CPE-mediated translational regulation during cell cycle, we analyzed the translational control driven by the UTRs from *Xenopus* cyclin B mRNAs. These mRNAs, containing putative CPEs and PBEs (Figures 1A and S1), are differentially regulated during meiotic progression (Hochegger et al., 2001).

All five cyclin mRNAs were stored as maternal silent mRNAs with short poly(A) tails in arrested oocytes (Figure 1A). In response to Prog stimulation, cyclin B1, B2, B4, and B5 but not B3 mRNAs were cytoplasmically polyadenylated. To better define the time of polyadenylation of these mRNAs after Prog stimulation, Cdc2 kinase activation and MI entry were blocked with cycloheximide (Chx), thus preventing "late" polyadenylation. It should be noted, however, that Chx also blocks multiple positive feedback loops, which have a significant effect reducing the length of the poly(A) tail. As shown in Figure 1B, the polyadenylation of both B1 and B4 endogenous mRNAs was completely abrogated by Chx treatment, indicating that both mRNAs are indeed polyadenylated "late" in a Cdc2-dependent manner. On the other hand, B5 mRNA polyadenylation, although reduced, was not blocked by Chx treatment indicating that this is an "early" Cdc2-independent polyadenylated mRNA. For B2 mRNA we observed what seemed to be a complete inhibition of the polyadenylation. However, because B2 mRNA displays

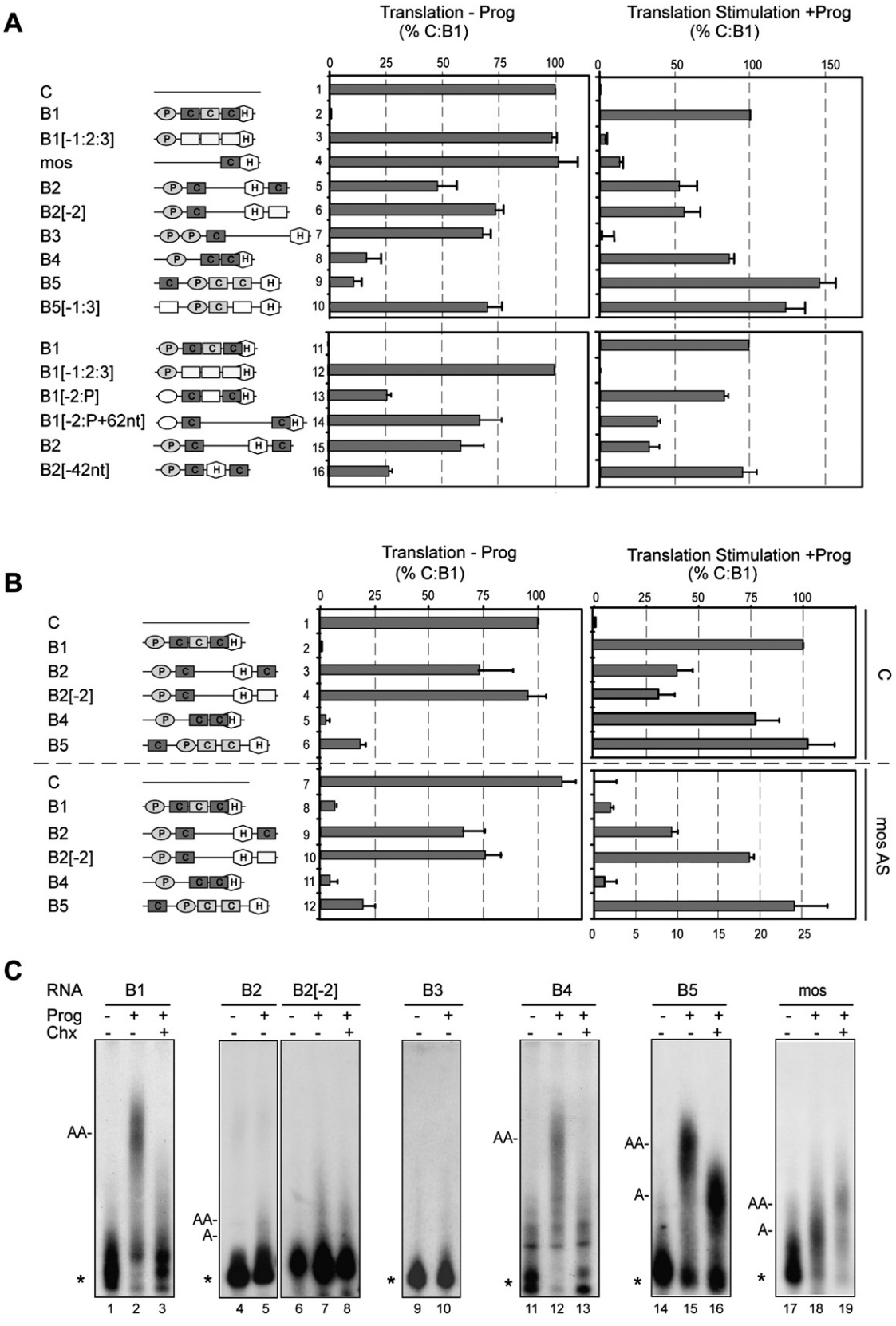
A
Translation - Prog
(% C:B1)
Translation Stimulation +Prog
(% C:B1)
C
B1
B1[-1:2:3]
mos
B2
B2[-2]
B3
B4
B5
B5[-1:3]
B1
B1[-1:2:3]
B1[-2:P]
B1[-2:P+62nt]
B2
B2[-42nt]
B
Translation - Prog
(% C:B1)
Translation Stimulation +Prog
(% C:B1)
C
mos AS
C
RNA
Prog
Chx
B1
B2
B2[-2]
B3
B4
B5
mos
AA-
A-
*

a lower polyadenylation than B5 it was possible that its early-reduced polyadenylation in the absence of feedback loops was not detectable by Northern blot. Therefore, we analyzed its polyadenylation by a higher-resolution technique based on RNA-ligation-coupled RT-PCR (Charlesworth et al., 2004). With this technique, both B5 and B2 polyadenylation, but not B1, were detectable in the presence of Chx, indicating that B2 is a weak "early" Cdc2-independent polyadenylated mRNA (Figure S2).

To analyze the role of cyclin B1–B5 3′UTRs on translational repression in prophase-arrested oocytes and on translational activation in response to Prog, cyclin B 3′UTRs, as well as mutant derivatives, were fused downstream of the firefly luciferase ORF (Figure S1). Identical amounts of the chimeric mRNAs were injected into stage VI oocytes then stimulated (translational stimulation) or not (translational repression) with Prog (Figure 2A). In both situations, the translational effect of the cyclin 3′UTRs was compared with a control 3′UTR of approximately the same length to account for nonspecific effects due to the 3′UTR length (Pique et al., 2006). Differences in mRNA stability were ruled out (Figure S3).

The repression effects were referred to cyclin B1 3′UTR (B1), which mediates a 5- to 10-fold translational repression in arrested oocytes (Figure S4). Translation of the nonrepressed control mRNA (C) was adjusted to 100% and that of the fully repressed B1 3′UTR reporter to 0% (Figures S4 and 2A, left panel). This repression was entirely dependent on the presence of functional CPEs as shown by disruption of all three CPEs by point mutation (B1[−1:2:3]). Of the other tested WT or variant 3′UTRs derived from cyclin B1–B5 and Mos mRNAs, only those containing a cluster of two or more CPEs (B4 and B5) efficiently mediated translational repression, whereas those 3′UTRs containing single CPEs such as B3, Mos, or a variant of B5 where two of the three CPEs were rendered not functional by point mutations (B5[−1:3]) had rather weak effects on translational repression. In B2, which contains two CPEs but 64 nts apart and one of them downstream of the Hex, repression was very weak, and only slightly affected by the inactivation of one of the two CPEs (B2[−2]). To distinguish whether the weak repression of B2 was due to the wide spacing between the two CPEs (64 nts) or to the fact that one CPE was downstream of the Hex, we tested a new B2 variant decreasing the distance between the two CPEs to 22 nt (B2[−42nt]). This variant mediated a stronger repression than its WT counterpart and similar to that obtained with the B1 variant with two CPEs, both upstream of the Hex (B1[−2:P]). Conversely, when in this B1 variant the distance between CPEs was increased up to 72 nts (B1[−2:P + 62nt]) by inserting a neutral sequence (Figure S5), the translational repression was reduced to levels similar to B2. Thus, we concluded that the distance between the CPEs and not their position respect to the Hex defines the extent of translational repression (Figure 2A).

The activation effects in response to Prog were also referred to the B1 chimeric mRNA, which was stimulated 30- to 40-fold in a CPE-dependent manner (Figure S4). The translational stimulation over a nonrepressed control was adjusted to 100% (Figure 2A, right panel). In agreement with the polyadenylation observed for endogenous mRNAs, all cyclin 3′UTRs stimulated the translation of the reporter with the exception of B3. A single CPE was sufficient to mediate translational activation as shown in B2 and B5 3′UTR variants containing single CPEs (B2[−2]) and B5[−1:3]), which displayed nearby the same degree of translational activation than their WT counterparts. However, the extent of translational activation was very different for all the tested 3′UTRs, with the lesser activation driven by Mos and the higher by B1, B4, and B5 3′UTRs, whereas B2 3′UTR displayed intermediate activity. These results suggest that features of the 3′UTR other than the sequence and number of CPEs regulate the extent of translational activation. Indeed, we observed a good correlation between the extent of translational activation and the distance between the CPE and the Hex. Thus, a CPE at 36 nts from the Hex, such as in B5(−1:3), correlated with a very efficient translational activation whereas larger separation, such as in B2(−2) (48 nts) or B3 (121 nts), reduced or abolished, respectively, polyadenylation and translational activation. This was further confirmed by a B1 variant where the distance between the CPE and the Hex was artificially increased to 76 nts (B1[−2:P + 62 nt]). This variant displayed a reduced translational activation, similar to B2. Conversely, a B2 variant where the distance between the CPE and Hex was reduced to 6 nts (B2[−42 nt]) displayed increased translational activation, similar to B1. Interestingly, a CPE adjacent to the Hex (Mos fragment) appeared also functionally impaired. Thus, the distance between the CPE and the Hex seems to modulate the extent of translational activation. The contribution of a CPE downstream of the Hex to activation is minor compared with a CPE upstream of the Hex (compare B2 versus B2[−2]).

To define the time of activation driven by each 3′UTR, Prog-induced Cdc2 activation was prevented with microinjected Mos-AS oligonucleotides (de Moor and Richter, 1997). As shown in Figure 2B, Mos ablation completely blocked translational activation mediated by B1 and B4 3′UTRs. However, B2 and B5 chimeric mRNAs were still activated. Interestingly, both B1 and B4 3′UTRs contain multiple CPEs, where one of them

Figure 2. Translational Control and Cytoplasmic Polyadenylation Mediated by Cyclin B1–B5 3′UTRs

(A) Translational regulation. Synthetic chimeric mRNAs containing the firefly luciferase coding sequence fused to a control 3′UTR (C), or to the indicated 3′UTRs, were coinjected with the renilla luciferase normalizing mRNA. Oocytes were then incubated in the presence or absence of Prog and collected 2 hr after maturation to determine the luciferase activity. The percent of translation in the absence of Prog for the different 3′UTRs with respect to control (100%) and B1 (0%) 3′UTRs is shown on the left panel. The percent of translation stimulation with Prog for the different 3′UTRs with respect to control (0%) and B1 (100%) 3′UTRs is shown on the right panel (see Figure S3). Data are represented as mean ± SEM. A schematic representation of the 3′UTRs, as in Figure 1, is shown on the left.

(B) Requirement of Cdc2 activation for translational stimulation. Oocytes, preinjected with Mos antisense oligonucleotide (Mos AS) overnight, were microinjected and treated as described above. Data are represented as mean ± SEM.

(C) Analysis of cytoplasmic polyadenylation. Oocytes were injected with the indicated radiolabeled 3′UTRs, treated with Chx and Prog as indicated and collected 2 hr after maturation of the control oocytes. Total RNA was extracted and analyzed by denaturing gel electrophoresis and autoradiography. Positions of the non-adenylated input RNAs (*), the maximal length of adenylated RNAs (AA), and the intermediate adenylated RNAs (A) are indicated.

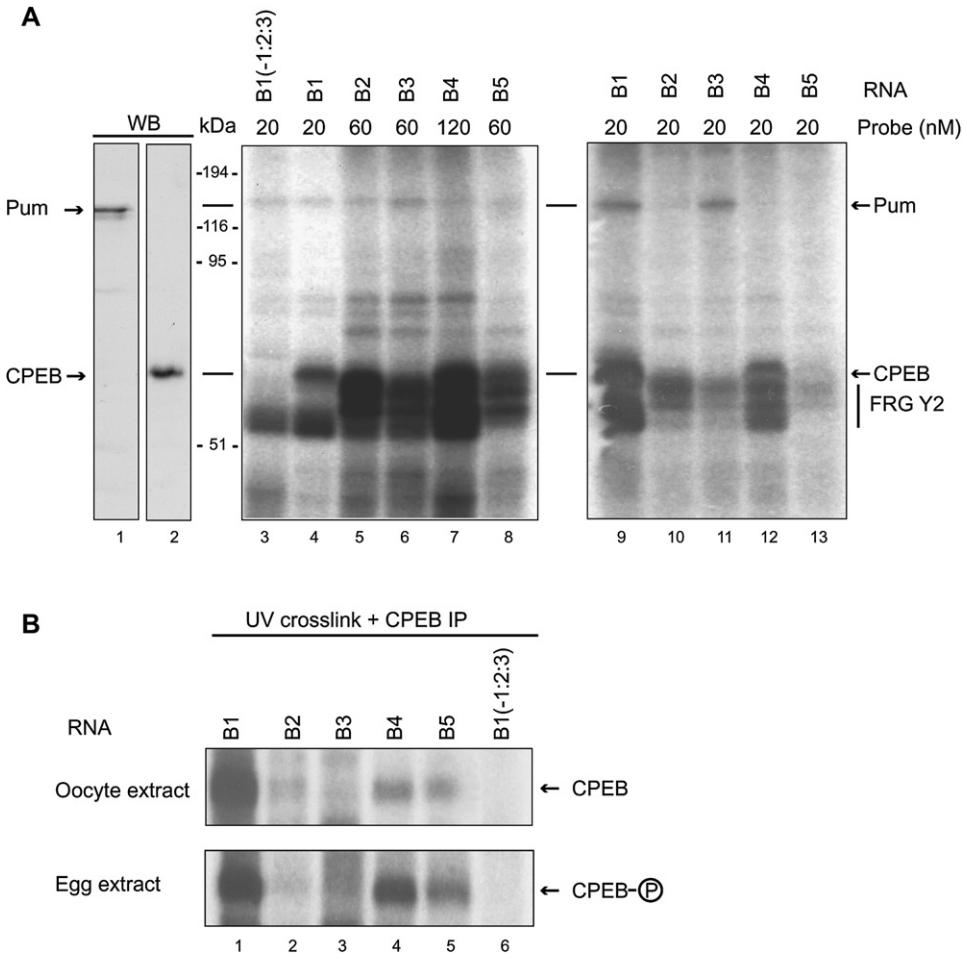

Figure 3. Analysis of CPEB and Pum Binding to Cyclin B1–B5 3′UTRs

(A) Extracts from stage VI oocytes were incubated with the indicated concentrations of radiolabeled 3′UTRs, UV-crosslinked, digested with RNase A, and visualized by autoradiography after 10% SDS-PAGE. On the left panel is shown a western blot analysis of two samples probed with anti-Pum (lane 1) and anti-CPEB (lane 2) antibodies.

(B) Immunoselection of CPEB-RNA complexes. Extracts from stage VI oocytes or eggs were incubated with the indicated radiolabeled 3′UTRs, UV-crosslinked, digested with RNase A, and then immunoprecipitated with CPEB antibody. The immunoselected CPEB was analyzed by SDS-PAGE and autoradiography. Bands corresponding to CPEB in oocyte extracts and CPEB hyperphosphorylated (CPEB-P) in egg extracts are indicated.

overlaps with the Hex, whereas the 3′UTRs that mediate Cdc2-independent translational activation do not contain an overlapping CPE. A similar picture emerged when cytoplasmic polyadenylation was directly visualized by microinjecting labeled cyclins B and Mos UTRs (Figure 2C). Thus, B1, B4, and B5 3′UTRs showed the strongest polyadenylation. B2 and Mos 3′UTRs displayed a very weak polyadenylation, whereas B3 3′UTR was not polyadenylated in response to Prog. When Cdc2 activation was blocked by the addition of Chx (Figure 2C), B1 and B4 polyadenylation were completely blocked, whereas B5 was still polyadenylated, if with a shorter poly(A) tail. B2 polyadenylation, although weak, was not prevented by Chx.

We next sought to determine whether the same factors were bound by all five cyclin B 3′UTRs, analyzed by UV crosslinking to UTP-labeled RNA substrates in oocyte extracts. Both CPEB and Pum are recruited to cyclin B1 3′UTR and have been identified as the most proximal factors mediating both the translational repression and activation of the mRNA (de Moor and Richter, 1999; Nakahata et al., 2003; Stebbins-Boaz et al., 1996). Indeed, two proteins comigrating with Pum and CPEB were crosslinked to B1 3′UTR (Figure 3A). The CPEB comigrating band was not detected when the CPEs were inactivated by point mutation (B1[−1:2:3]) and was immunoprecipitated with anti-CPEB antibody (Figure 3B). The Pum comigrating band was not detected when the PBE was mutated (B1[−P]) (Figure 4C). Both proteins were detected with labeled RNA substrates from all the cyclin UTRs (Figure 3A, middle panel). However, the crosslinking efficiency was very different for all five cyclin B 3′UTRs, and when equal molar amounts of RNA substrate were compared (Figure 3A, right panel), only B1 and B3 displayed a strong Pum crosslinking, whereas CPEB crosslinking was stronger for B1, B4, and B5 than for B2 and B3 (Figure 3B). FRGY2, a nonspecific RNA-binding protein with affinity for U-rich sequences (Murray et al., 1992), was also detected. These results revealed

a correlation between CPEB crosslinking and the ability of the 3′UTRs to mediate translational repression. No tight correlation was observed between Pum crosslinking and translational repression.

Analysis of the *cis*-Acting Elements Present in Cyclin B1 3′UTR

To further dissect the functional role of the *cis*-acting elements within the same 3′UTR context, we analyzed the combinatorial effects of the motifs present in cyclin B1 3′UTR on translation, polyadenylation, and binding of CPEB and Pum.

B1 3′UTR contains a PBE, two consensus CPEs (CPE1 and CPE3), and a putative nonconsensus CPE (CPE2) (Figures 1A and S1). When 3′UTRs derived from B1 mRNA were analyzed for their ability to repress translation of a luciferase reporter in arrested stage VI oocytes, only those that contained a combination of two or more CPEs (B1, B1[−1], B1[−2] and B1[−3]) mediated a significant repression whereas variants containing a single CPE (B1[−1:2], B1[−1:3], and B1[−2:3]) or no CPEs (B1[−1:2:3]) did not repress translation (Figure 4A, left panel). PBE inactivation in the presence of all three CPEs (B1[−P]) induced a moderate derepression as previously described (Nakahata et al., 2003), but the presence and absence of the PBE in the context of any of the variants with two CPEs or when combined with individual CPEs were consistently small. Thus, at least two CPEs are required to mediate translational repression, whereas the PBE has a minor effect. Moreover, the distance between the two CPEs defines the extent of repression with an optimal separation of 10–12 nts independently of the surrounding sequences (Figure S6).

When we analyzed Prog-mediated translational activation (Figure 4A, right panel), either CPE1 or CPE2 were sufficient to support translational activation of the reporter, although to different extents and with differential requirements for Pum. Thus, CPE1, (B1[−2:3]), induced an even greater stimulation than the WT 3′UTR, and this effect was reduced by half in the absence of PBE,(B1 [−2:3:P]). The nonconsensus CPE2, (B1[−1:3]), induced a similar activation but was much more sensitive to the PBE inactivation, (B1[−1:3:P]), which completely abolished translational activation. On the other hand, CPE3, (B1[−1:2]), did not support any translational activation regardless of the presence or absence of PBE. Moreover, the overlapping CPE3 itself seems to have an inhibitory effect over the translational activation mediated by the other CPEs (B1[−2:3] versus B1[−2], or B1[−1:3] versus B1[−1], or B1 versus B1[−3]). PBE inactivation, either in the WT (B1[−P]) or any of the variants with two CPEs, had no significant effect on the Prog-induced translational activation. Differences in luciferase activity were not due to differential stability of the reporter mRNAs (Figure S3). In summary, a single CPE is sufficient to support translational activation, and the distance between the CPE and the Hex defines the extent of activation with an optimal separation of 25 nts, independently of the surrounding sequences (Figure S6).

When this CPE is consensus, the activation is enhanced by the presence of a PBE or another CPE, but if the CPE is nonconsensus either of these additional elements are absolutely required. An overlapping CPE is not only nonfunctional in translation activation but has also a negative effect over upstream CPEs. Accordingly, when cytoplasmic polyadenylation was directly visualized (Figure 4B) by microinjecting labeled 3′UTRs, it was clear that single CPEs, such as CPE1 and CPE2 (B1[−2:3] and B1[−1:3]) mediate efficient polyadenylation but not CPE3 (B1[−1:2]), which overlaps with Hex. However, and in contrast to what was observed for the translational activation, PBE inactivation by point mutation did not have any effect on cytoplasmic polyadenylation, suggesting that PBE may have an additional role in CPE-mediated translational activation independent of poly(A) tail elongation.

To confirm that PBE and the three CPEs were indeed functional elements capable of recruiting, respectively, Pum and CPEB, we performed UV-crosslinking analysis (Figure 4C) of B1 3′UTR (B1), a variant with PBE inactivated (B1[−P]), a variant with all three CPEs inactivated (B1[−1:2:3]) or variants with each of the individual CPEs in the presence or absence of PBE. UV crosslinking with B1 showed labeling of Pum and CPEB only when the respective elements, PBE and CPE, were present. When labeled probes for the 3′UTR variants containing single CPEs were analyzed, only CPE1 yielded a significant CPEB binding, which was not affected by the presence or absence of PBE. Under these conditions, CPE2 and CPE3 produced no detectable signal and CPEB labeling by Mos 3′UTR probe was also weak. Only by doubling the amount of probe, CPEB labeling was detected for CPE2 and CPE3 but now, in contrast to CPE1, labeling was dependent on the presence of PBE. Note that the label CPEB crosslinked to WT B1 was stronger than the addition of the CPEB crosslinked to individual CPEs, suggesting the possibility of cooperative binding.

In order to determine whether complexes containing multiple CPEBs and Pum were assembled in B1, the WT and variant UTRs were used as RNA probes for gel-shift experiments. With the WT probe and in the presence of a high concentration of extracts (5 mg/ml), four specific complexes were detected (Figure 5A). A and B contained CPEB because they were not present when a B1 variant probe that did not contain CPEs was analyzed. According to the mobility and competition assays (see below), F most likely corresponds to FRGY2. When a B1 variant RNA that does not contain PBE was analyzed, A, B, and C were not present indicating that these complexes contained Pum. Moreover, in the absence of PBE two new shifted species appeared, D and E, which correspond to CPEB complexes without Pum. In addition, when a B1 variant containing a single CPE in the presence of PBE (CPE1) was analyzed, B and C were detected but not A, D, or E and, in the absence of PBE, only E was detected but not A, B, C, or D. Taken together, these data suggested that A corresponded to a complex containing two CPEBs and Pum and B reflected the formation of a complex containing Pum and a single CPEB, whereas D was a complex containing two CPEBs. C and E corresponded, respectively, to complexes containing single Pum and CPEB molecules. When a lower extract concentration was used in the assay (1.25 mg/ml) to make *trans*-acting factors limiting, the A and D shifted bands were not detected, suggesting that CPEB but not Pum was the limiting factor in the formation of high order complexes. This situation may reflect what happens in oocytes at MI when most of the CPEB is degraded (Mendez et al., 2002).

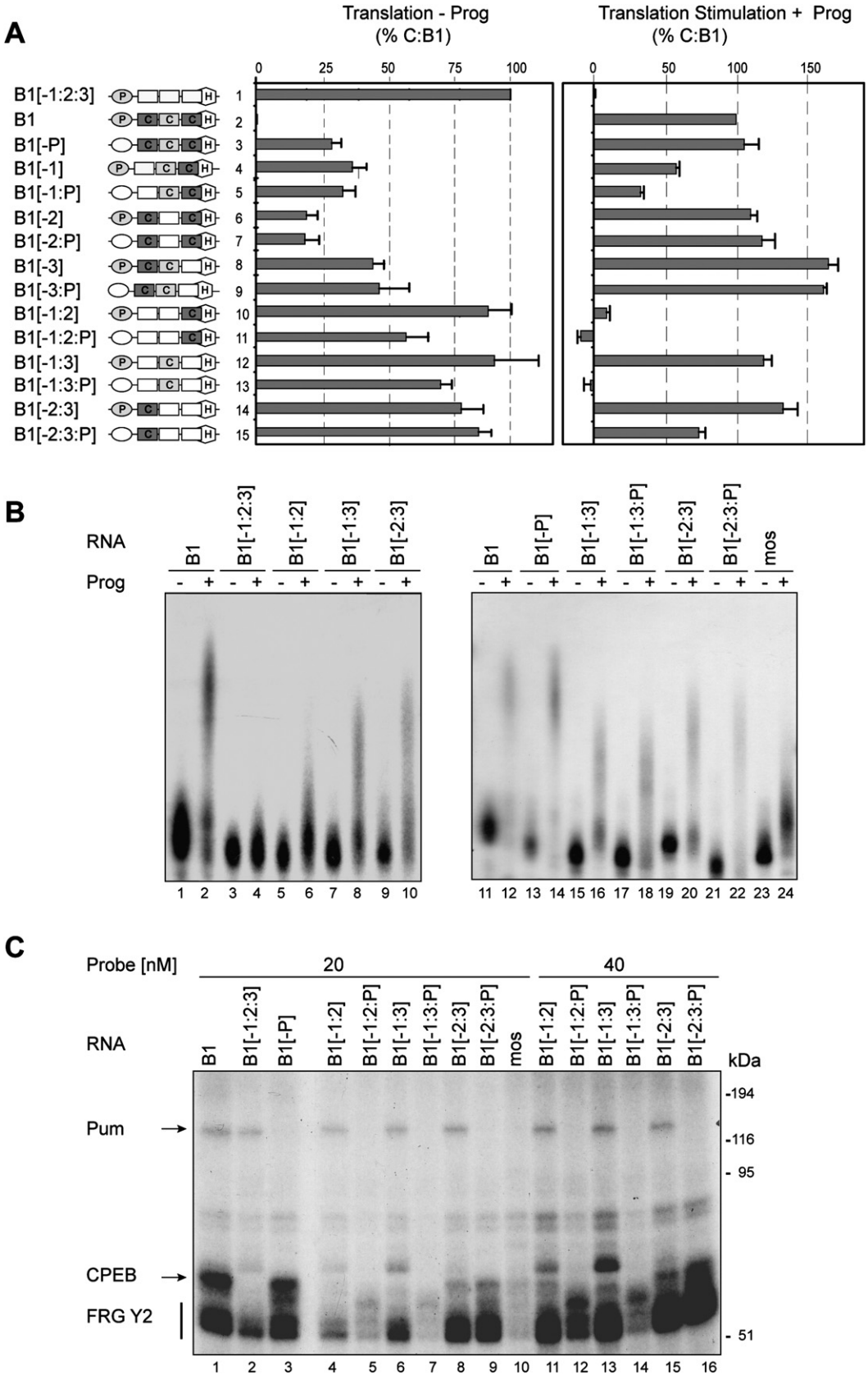
A
Translation - Prog
(% C:B1)
Translation Stimulation + Prog
(% C:B1)
0
25
50
75
100
150
B1[-1:2:3]
B1
B1[-P]
B1[-1]
B1[-1:P]
B1[-2]
B1[-2:P]
B1[-3]
B1[-3:P]
B1[-1:2]
B1[-1:2:P]
B1[-1:3]
B1[-1:3:P]
B1[-2:3]
B1[-2:3:P]
1
2
3
4
5
6
7
8
9
10
11
12
13
14
15
B
RNA
Prog
B1
B1[-1:2:3]
B1[-1:2]
B1[-1:3]
B1[-2:3]
B1[-P]
B1[-1:3:P]
B1[-2:3:P]
mos
1 2 3 4 5 6 7 8 9 10
11 12 13 14 15 16 17 18 19 20 21 22 23 24
C
Probe [nM]
20
40
RNA
B1
B1[-1:2:3]
B1[-P]
B1[-1:2]
B1[-1:2:P]
B1[-1:3]
B1[-1:3:P]
B1[-2:3]
B1[-2:3:P]
mos
kDa
-194
-116
- 95
- 51
Pum
CPEB
FRG Y2
1 2 3 4 5 6 7 8 9 10 11 12 13 14 15 16

To further characterize the identity of these complexes, we performed gel-shift competition assays with the lower extract amount (1.25 mg/ml) and B1 as RNA probe (Figure 5B). The assay was performed in the presence of increasing amounts of cold control RNA or B1 variants, either with CPE1 and Hex, with PBE and Hex or with Hex alone. As expected, the CPE-containing RNA efficiently competed the B-shifted band and the PBE-containing RNA competed both B and C. On the contrary, neither the B1 3′UTR derived RNA without any CPE or PBE nor the control RNA showed any competition. Moreover, supershift experiments in the presence of anti-CPEB, anti-Pum, or control IgG antibodies showed that the Bcomplex was disrupted by anti-CPEB antibody and supershifted by anti-Pum antibody, further confirming the identity of this complex. Complex C was also supershifted by anti-Pum antibody if to a lesser extent than complex B (Figure 5C).

To determine if the detected complexes displayed a differential stability on the RNA that may explain their differential translational effects, we performed competition experiments where the competitor RNAs were added after the B1 or B1(−P) 3′UTRs/protein complexes were already assembled. Under these conditions, a competitor RNA containing a single CPE was able to efficiently dissociate the D and E RNA-protein complexes containing, respectively, one or two CPEBs, but not the CPEB-Pum containing A complex, indicating that Pum stabilizes CPEB on the target mRNA (Figure 5D).

Thus, all three CPEs, consensus and nonconsensus, recruited CPEB although the efficiency of crosslinking was higher for CPE1 than for CPEs 2 and 3. Multiple CPEs were simultaneously occupied in what seems to be a cooperative manner. Finally, Pum appears to stabilize the CPEB bound to the RNA.

Determinants of "Early" Versus "Late" Cytoplasmic Polyadenylation-Dependent Translational Activation

To define the combination of elements that determined the "late" translational activation of cyclin B1, we compared the Prog-induced translational stimulation mediated by B1 variants in the presence or absence of Cdc2 activation. B1 translational activation was completely abolished in the absence of Mos (Figures 6A and 2B) indicating that translational activation was late (i.e., Mos and Cdc2-dependent). However, when CPE2 and CPE3 were inactivated by point mutations, (B1[−2:3]), translational activation was maintained in the absence of Mos suggesting that CPE2 or CPE3 were responsible for the "late" activation. Indeed, CPE3 was sufficient to confer "late" activation to the translation driven by CPE1. CPE3 overlaps with Hex and was nonfunctional in translational activation or cytoplasmic polyadenylation by itself (Figures 4A and 4B). Thus, translational activation was mediated in both cases by the CPE1, but when CPE3 was present the activation was Cdc2-dependent. This result was compatible with two different mechanisms, (1) a cluster of two CPEs was required to confer the Cdc2 dependence and (2) the overlapping CPE inhibited the "early" activation mediated by CPE1. To test these possibilities we increased the distance between the CPE3 and the Hex to 0 (B1[0 nt]) or 7 (B1[7 nt]) nts (Figure 6A). The variant B1(7 nt) in the presence of Mos AS clearly showed an early activation. The variant B1(0 nt) displayed a biphasic activation, with a very weak early activation and a strong late activation. Conversely, when B5 was modified by adding an additional CPE overlapping with Hex (B5[+CPEov]), it was converted from an early to a late activated 3′UTR.

A similar pattern appeared when the polyadenylation of the labeled 3′UTRs was analyzed in the presence of Chx to prevent Cdc2 activation in response to Prog (Figure 6B). Thus, the polyadenylation of those 3′UTRs with a CPE overlapping the Hex, such as B1 or B5(+CPEov), was blocked by Chx, whereas those UTRs without an overlapping CPE, such as B1[−2:3], B1(7 nt) or B5, were still polyadenylated. The variant B1(0 nt) displayed again an intermediate effect. Thus, the presence of a CPE overlapping with Hex conferred the late activation profile to a 3′UTR containing another upstream functional CPE. Although, it should be noted that on its own it is not sufficient to support neither early nor late polyadenylation.

Identification of CPE-Mediated Translational Control Motif Patterns across Vertebrate Genomes and Experimental Validation

Based on the behavior of the *Xenopus* cyclin B1–B5 mRNAs, we have experimentally defined a combinatorial code for CPE-mediated translational regulation, which is schematized in Figure S7. In this code, 24 configurations of the basic *cis*-acting elements (CPE, Hex, and PBE) define 6 different modes of translational behavior. In an attempt to assess the generality of this code, we performed a genome-wide computational search for the occurrence of these configurations in the 3′UTRs of human, mouse, and *Xenopus* mRNAs, and randomly selected a few cases for experimental validation of the predicted translational behavior. To perform the search, the experimentally derived motifs were represented as regular expressions to infer instances of motif configurations from the individual motif matches (see Supplemental Data). Thirty to forty-five percent of all analyzed UTRs harbor at least one of the configurations predicted to be involved in CPE-mediated translational regulation (Table S1). Gene Ontology analysis shows that the human- and mouse-predicted CPE-regulated mRNAs are significantly enriched in transcripts encoding for proteins with a biological function related to cell cycle and cell differentiation (Table S2).

Figure 4. Combinatorial Contributions of CPEs and PBE to the Translation Control and Cytoplasmic Polyadenylation Driven by Cyclin B1 3′UTR

(A) Analysis of translation. Synthetic chimeric mRNAs containing the firefly luciferase coding sequence fused to the indicated cyclin B1 3′UTRs were examined for translation in presence or absence of Prog as in Figure 2A. Data are represented as mean ± SEM.

(B) Analysis of polyadenylation. The indicated radiolabeled cyclin B1 and Mos 3′UTRs were injected into oocytes and analyzed for cytoplasmic polyadenylation as in Figure 2C.

(C) Analysis of CPEB and Pum binding. Extracts of stage VI oocytes were incubated with the indicated concentrations of radiolabeled 3′UTRs, UV-crosslinked, digested with RNase A, and visualized by autoradiography as in Figure 3A.

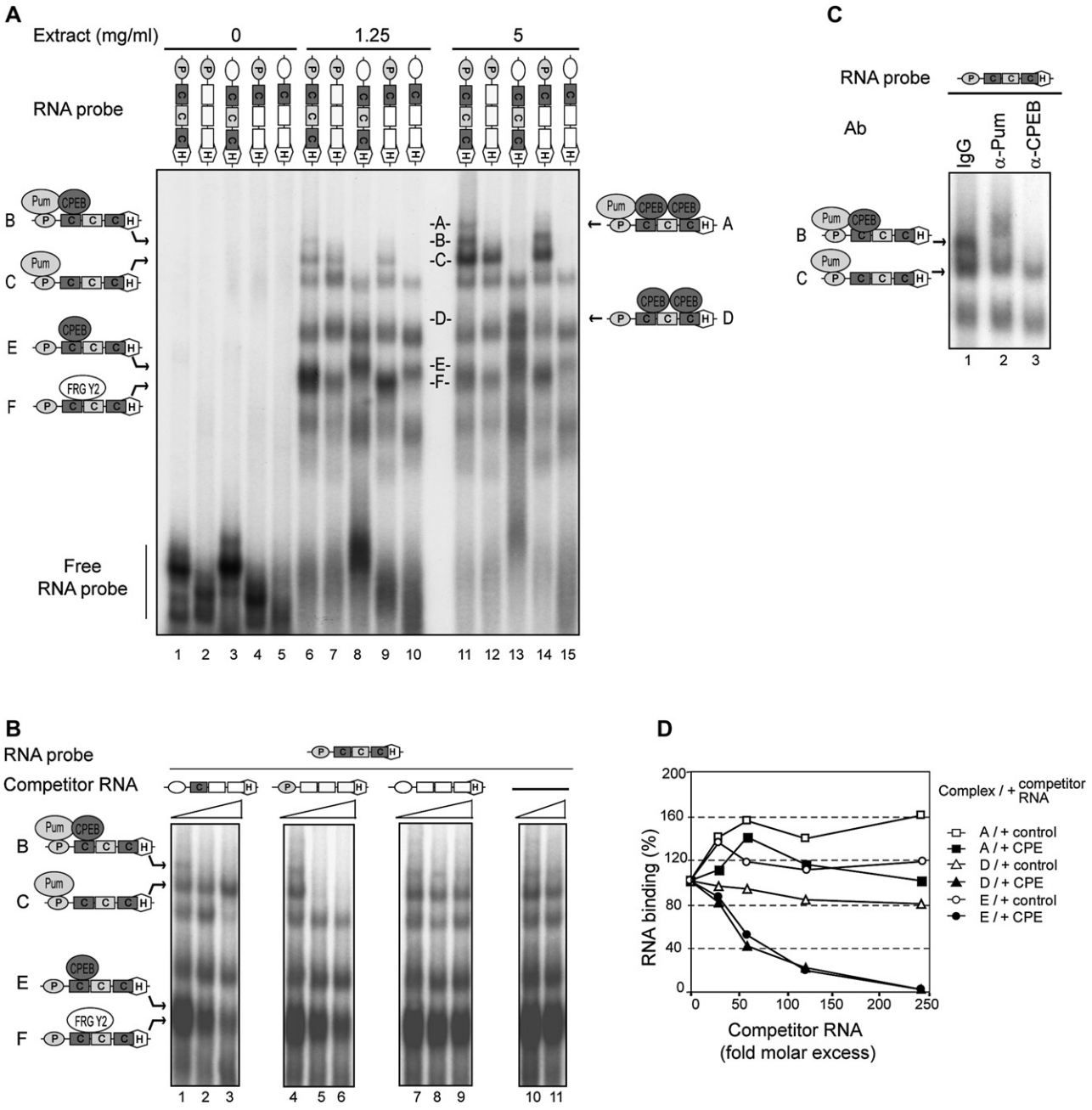

Figure 5. Analysis of the Complexes Recruited by Cyclin B1 3′UTR

(A) Identification of the CPEB and Pum-containing complexes. The indicated radiolabeled 3′UTRs were incubated with different concentrations of cytoplasmic extracts of stage VI oocytes (0, 1.25, or 5 mg/ml) and analyzed by gel retardation assays. A schematic representation of each of the RNA-protein complexes containing Pum, CPEB, and FRG Y2 is shown.

(B) Gel-shift competition assay. Oocyte extracts (1.25 mg/ml) were incubated first with the unlabeled competitor RNAs at 0-, 30-, and 100-fold molar excess and then radiolabeled cyclin B1 3′UTR was added. RNA-protein complexes are indicated.

(C) Supershift assay in the presence of anti-CPEB, anti-Pum, or control IgG antibodies. RNA-protein complexes are indicated.

(D) Analysis of stability of the complexes bound to cyclin B1 3′UTR. Oocyte extracts (5 mg/ml) were preincubated with the indicated radiolabeled 3′UTRs to assemble RNA-protein complexes. Then, the indicated unlabeled RNA competitors were added at 0-, 30-, 60-, 120-, and 240-fold molar excess. Graph represents densitometric quantification of bands A, D, and E expressed as percentage of the uncompeted.

To confirm experimentally the specific association that we postulate between motif configurations and translational behavior, we randomly selected 27 mRNAs that were present in both human and mouse 3′UTR within the same translational control group. We attempted to cover as many different translational behaviors as possible by randomly selecting from all the different

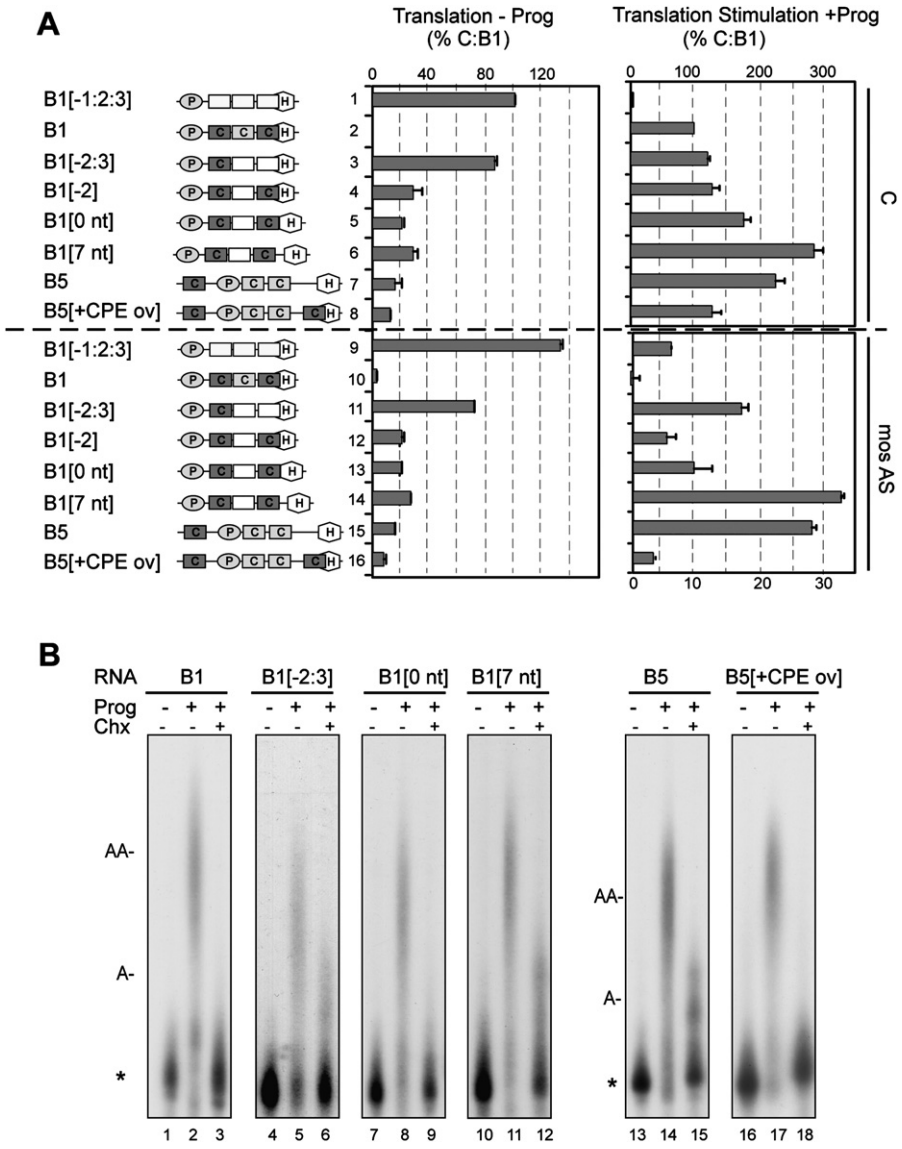

Figure 6. Determinants of the Late Translational Activation and Cytoplasmic Polyadenylation

(A) Analysis of translation. Translation of synthetic chimeric mRNAs containing the firefly luciferase coding sequence fused to the indicated cyclins B1 and B5 3′UTRs were examined in the presence or absence of Mos AS, as in Figure 2B. A schematic representation of the 3′UTRs is shown on the left, as described in Figure 2A. Data are represented as mean ± SEM.

(B) Analysis of polyadenylation. Cytoplasmic polyadenylation of the indicated radiolabeled cyclins B1 and B5 3′UTRs injected in oocytes, pretreated or not with Chx, was analyzed as in Figure 2C.

categories in different combinations (Figure 7B and Table S3). Because continuous quantitative effects defined by the distances between the CPE-CPE (for repression) and CPE-Hex (for activation) motifs were translated into discrete groups by imposing cut-offs, we qualified the predictions tested in Figure 7B by adding arrows indicating whether we predicted this UTR to fall in the upper, middle, or lower range of each category. The selected 3′UTRs were analyzed for their ability to repress translation as well as to stimulate translation in the presence or absence of Cdc2 kinase activity. The repression predictions were qualitatively and quantitatively accurate for all the UTRs except for UTR8 although the deviation from the repression threshold (7%) was smaller than the experimental variation. The activation predictions were correct for most of the UTRs, with the exceptions of UTRs 1, 2, 20, 24, and 27, although for the UTR 20 the deviation from the activation threshold was within the experimental variation for this reporter. The predicted timing of activation was correct, with the exception of UTRs 7, 9, and 17. The deviation for the first two was less than 5% from the predicted threshold. These subtle changes are probably related to the large number of CPEs present in these UTRs that could somehow slow down the activation. Indeed, deletion of the three

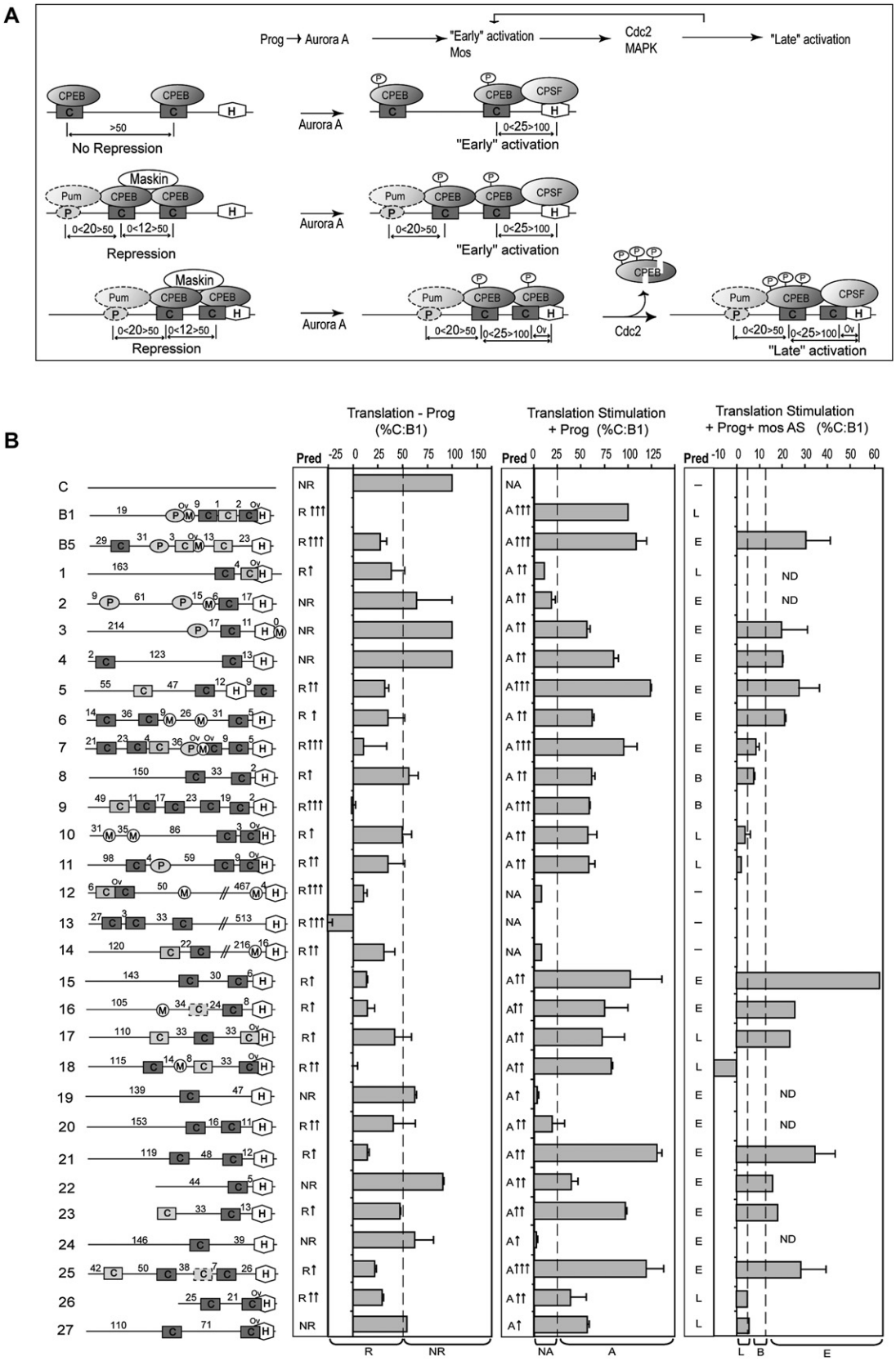
A
Prog → Aurora A
"Early" activation
Mos
Cdc2
MAPK
"Late" activation
CPEB
CPSF
Maskin
Pum
No Repression
Repression
Aurora A
"Early" activation
Cdc2
"Late" activation
B
Translation - Prog
(%C:B1)
Translation Stimulation
+ Prog (%C:B1)
Translation Stimulation
+ Prog+ mos AS (%C:B1)
Pred
R
NR
NA
A
L
B
E
ND

upstream CPEs of UTR9 made the biphasic behavior more clearly appreciable (9-Δ1, Figure S8).

To determine whether, for the UTRs that did not behave as predicted, additional regulatory elements could be obscuring the CPE-mediated translational regulation, we performed a more detailed analysis of UTR1 and UTR2. Serial deletions and point mutations in UTR1 indicate that the lack of activation in response to progesterone was due to an additional *cis*-acting element (GAUCU) that blocked activation (1-Δ6, Figure S8). The failure of UTR2 to activate translation as predicted was derived from the long palindromic region upstream of the CPEs, which is predicted to form a very stable secondary stem-loop structure (−15 kcal/mol, M fold) containing an RNA secondary structure motif K turn (Klein et al., 2001). Accordingly, deletion of this region resulted in UTR2 being translationaly activated (2-Δ1, Figure S8). Thus, the overall successful prediction rate for CPEB-mediated translational repression was 96.3%, for CPE-mediated activation was 92.5%, and for the time of activation 89.4%.

DISCUSSION

The analysis of the polyadenylation state of the endogenous cyclin mRNAs during meiosis, the capability of their 3′UTRs to direct translational repression and subsequent cytoplasmic polyadenylation and translational activation of a reporter, as well as the analysis of the *trans*-acting factors assembled on specific *cis*-acting elements, allowed us to define a set of rules that can be used to predict the translational behavior of CPE-containing mRNAs in a qualitative and quantitative manner. These rules are based on the different combinations of a limited number of *cis*-acting elements (the Hex, CPEB, and PBE).

Translational Repression

CPE-mediated translational repression requires a cluster of at least two CPEs, irrespective of its position along the 3′UTR, where the distance between the pair of CPEs defines the repression efficiency with and optimal separation of 10–12 nt (Figure S6). Thus, only the WT forms of B1, B4, and B5 3′UTRs, the B1 variants with two CPEs, and the B2 variant with a reduced distance between the CPEs were able to mediate translational repression (Figures 2 and 4). However, 3′UTRs with two distant CPEs, like B2 and the B1 variant with increased distance between the CPEs, or 3′UTRs with a single CPE, like B3 and variants of B1, B2, and B5, were not able to induce repression of translation. Interestingly, only a cluster of CPEs as in B1 or B4 promotes a cooperative CPEB binding, whereas for distant CPEs as in B2 the binding seems merely additive over single CPEs (Figures 3 and 4C). These results explain previous observations for Mos, cyclins A1 and B1, Wee1, GLD-2, or artificial 3′UTRs (Barkoff et al., 2000; Charlesworth et al., 2000; de Moor and Richter, 1999; Rouhana and Wickens, 2007). In addition, we show that PBE increased the repression, mediated by a cluster of three CPEs, by 2-fold (Figure 4A) in concordance with previous results (Nakahata et al., 2003). However, neither a PBE alone nor a PBE together with one or two CPE(s) had any effect on repression (Figure 4A), which may reveal an effect of Pum to position the repressor CPEB dimer in the more efficient CPEs 1 and 3.

These results are consistent with a model where the repression would be mediated by a heterotrimer of Maskin and two CPEBs rather than multiple CPEB-Maskin heterodimers.

Cytoplasmic Polyadenylation and Translational Activation

CPE-mediated cytoplasmic polyadenylation and translational activation requires a single consensus CPE and the distance between this element and Hex modulates the extent of polyadenylation and translational activation with an optimal distance of 25 nts (Figure S6). Thus, a CPE from 6 (B1[−1:3] and B2[−42nt]) to 14 (B1[−2:3]) or 23 (B5) nts induces maximal activation. Increased distances, such as 48 (B2[−2]) or at 76 (B1[−2:P + 62 nt]) nts from the Hex induces a weak polyadenylation and translational activation, whereas at 121 nts (B3) is nonfunctional (Figure 2). A much more fine-tuned control of the extent of activation is accomplished by decreasing the distance from CPE to Hex. Thus, a CPE just adjacent (Mos or B1[0 nt]) reduced the stimulation up to 10-fold, while a CPE overlapping with Hex is not only nonfunctional in translational activation, but has a negative effect over upstream CPEs (Figure 4). These results explain previous observations for histone-like B4, Cdc1, cyclin A1, and G10 (Sheets et al., 1994; Stebbins-Boaz et al., 1996). The number of CPEs has also an effect on the extent of activation but is not even additive. Surprisingly, Pum has a much stronger effect on translational activation than on repression. Thus, a PBE in conjunction with a single consensus CPE enhances translation by 2-fold (Figure 4). When acting together with the nonconsensus CPE2, the PBE becomes absolutely required. The effect of the PBE is probably due to the stabilization of CPEB on the mRNA (Figure 5D), and, accordingly, in the context of a CPEB dimer (B1[−3]), removal of the PBE has no effect. Interestingly, the effect of PBE on CPE-mediated translational activation did not reflect the degree of polyadenylation, indicating that polyadenylation may be required but not sufficient to

Figure 7. Model for CPE-Mediated Translational Control and Experimental Validation of Predicted CPE-Regulated 3′UTRs

(A) Schematic representation of the *cis* elements and *trans*-acting factors recruited, with their covalent modifications. The distances required to mediate translational repression and activation as well as the time of activation are indicated. Optional factors/elements are displayed with dotted lines.

(B) Synthetic chimeric mRNAs containing the firefly luciferase coding sequence fused to the indicated 3′UTRs derived from *X. laevis* cyclin B1 (B1), cyclin B5 (B5), and *M. musculus* 3′UTRs numbered from 1 to 27 (for identity and accession number, see Supplemental Data) were injected into oocytes and analyzed for translation as in Figures 2A and 2B. A schematic representation of the structure of the 3′UTRs is shown on the left (according to Figure 1, dotted boxes indicate putative CPEs). The predicted translational effect (Pred), both in repression (R) and activation (A), the timing of activation (Early, E; late, L; and Biphasic, B) for each 3′UTR is shown on the left of each graph. NR and NA stand for nonrepression and nonactivation, respectively. Arrows indicate the predicted strength of the effect. The dotted line establishes the threshold for repression, activation, and cdc2-independent activation of translation. A schematic representation of the 3′UTRs, as in Figure 1, is also shown. Potential Musashi binding sites are also depicted (M). ND, not determined.

stimulate translation of CPE-containing mRNAs and that CPEB would increase translation by other mechanism that requires a "stronger" binding than CPSF recruitment.

Temporal Cytoplasmic Polyadenylation Determinants

The defining feature of late cytoplasmic polyadenylation is the presence of a CPE overlapping with Hex. Thus, the early or Cdc2-independent cytoplasmic polyadenylation is driven by a single CPE or by a cluster of CPEs nonoverlapping with Hex, whereas the late or Cdc2-dependent polyadenylation requires at least two CPEs, with one of them overlapping with Hex. This was suggested by the results presented in Figure 2, where 3′UTRs that contained a CPE plus an overlapping CPE, B1, and B4, displayed a late pattern of polyadenylation and translational activation, whereas B5 was polyadenylated early. These observations were confirmed (Figure 6) when the inactivation or displacement of the overlapping CPE from B1 turned this mRNA into an early polyadenylated messenger and, conversely, the addition of an overlapping CPE into the 3′UTR of B5 changed this mRNA from early to late polyadenylation. From the combination of the regulation of time and extent of activation emerges a new group of mRNAs displaying a biphasic behavior. These mRNAs show a weak polyadenylation in the early phase but a strong polyadenylation in the late phase. This class is characterized by an UTR with a downstream CPE at a suboptimal distance of the Hex (0–2 nt) and another upstream CPE at an optimal distance from the Hex (10–20 nt). These rules explain previous reports for the late Wee1 and cyclins A1, B1, and B4 mRNAs, and early cyclin B2, histone-like B4, D7, Eg2, FGFR1, G10, c-Mos, Cdc1, Eg3, XBub3, and GLD-2 mRNAs (Sheets et al., 1994; Stebbins-Boaz et al., 1996; Ballantyne et al., 1997; Charlesworth et al., 2004; Charlesworth et al., 2000, 2006; de Moor and Richter, 1997; Rouhana and Wickens, 2007).

We did not observe any clear correlation between the presence of the PBE and late polyadenylation, nor with the presence of the Musashi binding motif and early polyadenylation. B1 variants can be converted from late to early all in the presence of PBE (Figure 6). The Musashi binding motif (Figures S1 and 7B) is present in a number of late, early, and nonactivated UTRs. Noteworthy, many early-activated UTRs do not contain a Musashi-binding motif. Moreover, the temporal behavior of cyclin B1 and B5 UTRs can be modified by changing the arrangement of CPEs without affecting the Musashi binding motif (Figure 6).

We concluded that both early and late polyadenylation are mediated by CPEB, but the levels of this protein define when the late polyadenylated mRNAs will be activated (Figure 7A). This effect is directly mediated by the fact that a CPE overlapping with the Hex has a dominant-negative effect in polyadenylation, and subsequent translational activation (Figure 4) detected only in the presence of high CPEB levels. Thus, during the PI to MI transition, where the levels of CPEB are very high, multiple CPEs are occupied, including the one overlapping the Hex (Figure 5A), preventing the recruitment of CPSF to the Hex. However, after Cdc2 is activated at MI most of the CPEB is degraded (Mendez et al., 2002) and stochastically only one CPE would be occupied (Figure 5A). Because the nonoverlapping CPE has a higher affinity for CPEB than the overlapping CPE-Hex (Figure 4C) that would imply that now the single CPEB would be preferentially recruited to CPE and free to recruit CPSF to the Hex and promote polyadenylation (Figure 7A).

Altogether, this study defines a combinatorial code where the number and relative position of two elements, CPE and Hex, determine whether an mRNA will be translationally repressed by CPEB or not as well as the extent and time of cytoplasmic polyadenylation-dependent translational activation. From the data presented in this study a set of rules can be derived (Figures 7A and S7): (1) Translational repression requires a cluster of at least two CPEs, irrespective of its position along the 3′UTR, where the distance between adjacent CPEs defines the extent of repression with an optimal distance of 10–12 nts. (2) Translational activation requires, at least, a single consensus CPE or a nonconsensus CPE together with a PBE. The CPE must be closer than 100 nts from the Hex, but not overlapping. (3) The distance CPE-Hex determines the extent of polyadenylation and translational activation, with an optimal distance of 25 nts. Additional PBEs or CPEs have a positive effect except for an overlapping CPE, which has a negative effect. (4) Early or Cdc2-independent cytoplasmic polyadenylation requires CPE(s) nonoverlapping with the Hex, whereas late or Cdc2-dependent polyadenylation is driven by at least two CPEs, with one of them overlapping the Hex.

To determine whether we could predict the translational fate of mRNAs, we performed a computational analysis, identifying the appearance of these combinatorial motif patterns in vertebrate 3′UTRs. We identified hundreds of mRNAs, enriched for genes functionally related to cell cycle and cell differentiation regulation, potentially regulated by CPEB (Tables S1 and S2). We randomly chose 27 of them, corresponding to different translational control groups, and we successfully verified their predicted translational regulatory pattern (Figures 7B and S8). Our results indicate, thus, that this combinatorial code could serve as a general molecular language to define, qualitative and quantitatively, whether a given mRNA could be a target for cytoplasmatic polyadenylation control. Taking the full mechanistic meaning of the terms early and late (i.e., early: mediated by Aurora A kinase but independent of Cdc2 and the levels of CPEB; late: mediated by both Aurora A and Cdc2 and the subsequent low levels of CPEB), the conclusions of our work seem fully extrapolable to other systems beyond *Xenopus* oocyte maturation. Indeed, many genes are potentially regulated by CPEB and are implicated in a variety of biological functions, mainly related to cell cycle and cell differentiation but also to other biological events such as chromosome segregation, synaptic stimulation, embryonic polarity, or even implicated in angiogenesis and tumor development, etc. Accordingly, the proportion of 3′UTRs containing CPE-mediated translation control motif configurations is significantly higher than the proportions of 5′UTRs or control UTRs generated by randomly reassigning the position of the nucleotides or the positions of the detected *cis*-acting motifs for each 3′UTR (Table S4). Comparative analysis across 17 vertebrates shows that CPEs predicted to be involved in translational regulation are more conserved than those which are in nonregulatory positions (Figure S9), suggesting the presence of selective constraints for the regulatory arrangements of CPE-motifs.

EXPERIMENTAL PROCEDURES

Oocyte and Egg Preparation

Stage VI oocytes were obtained from *Xenopus laevis* females and induced to mature with progesterone (10 μM, Sigma) as described (de Moor and Richter, 1999). When required, oocytes were treated with Cycloheximide (0.35 mM, Sigma) or microinjected with Mos antisense oligonucleotide (0.02 nmols/oocyte) (Sagata et al., 1988). Eggs were obtained as described (Hake and Richter, 1994).

Northern Blot Analysis

Total RNA was purified and analyzed by northern blot as described (de Moor and Richter, 1997). Specific DNA probes for *X. laevis* cyclin Bs were labeled by random priming. When indicated, RNA samples were treated with RNase H and oligo d(T) (30 pmols per reaction) prior to northern analysis.

Analysis of the Translational Control and Cytoplasmic Polyadenylation by 3′UTRs

The radiolabeled or free-labeled competitor 3′UTRs, firefly luciferase/3′UTRs plasmids, and the normalizing plasmid pRenilla were generated as described (Pique et al., 2006) (for 3′UTRs sequences, see Supplemental Experimental Procedures).

For translation, oocytes were microinjected with 0.025 fmols of each hybrid reporter mRNA. For polyadenylation assays, oocytes were injected with 4.6 fmols of radiolabeled 3′UTR RNAs and analyzed as previously described (de Moor and Richter, 1997).

UV Crosslinking, Immunoprecipitation, Western Blotting, and RNA Electrophoretic Mobility Shift Assays

UV crosslinking and RNA gel retardations were performed as described (de Moor and Richter, 1999). For Western blot, anti-CPEB (Hake and Richter, 1994) or anti-Pum (Nakahata et al., 2003) antibodies were used as described.

In Silico Analysis

The 3′UTR sequences for the species analyzed were extracted from the NCBI Reference Sequences (RefSeq). *Cis*-acting motifs were represented as regular expressions, and searched for matches on UTR sequences by in-house developed PERL scripts. A program was implemented to assign mRNAs to translational regulation classes based on the predicted matches to *cis*-acting motifs. Functional analysis was performed according to the functional annotations provided by the Gene Ontology project . For detailed information on the "in silico" analysis see Supplemental Data.

Supplemental Data

Supplemental Data include nine figures, three tables, Supplemental Experimental Procedures, and Supplemental References and can be found with this article online at http://www.cell.com/cgi/content/full/132/3/434/DC1/.

ACKNOWLEDGMENTS

We thank Joel Richter and Masakane Yamashita for antibodies; Fátima Gebauer for the reporter plasmids pLuccassette and pRenilla and her helpful discussions; and Mercedes Fernández, members of the Méndez laboratory, and Juan Valcárcel for helpful advice and critically reading the manuscript. This work was supported by grants from the MEC, Fundación "La Caixa," and Fundació "Marató de TV3."

Received: August 9, 2006
Revised: October 31, 2007
Accepted: December 20, 2007
Published: February 7, 2008

REFERENCES

Ballantyne, S., Daniel, D.L., Jr., and Wickens, M. (1997). A dependent pathway of cytoplasmic polyadenylation reactions linked to cell cycle control by c-mos and CDK1 activation. Mol. Biol. Cell *8*, 1633–1648.

Barkoff, A.F., Dickson, K.S., Gray, N.K., and Wickens, M. (2000). Translational control of cyclin B1 mRNA during meiotic maturation: coordinated repression and cytoplasmic polyadenylation. Dev. Biol. *220*, 97–109.

Barnard, D.C., Ryan, K., Manley, J.L., and Richter, J.D. (2004). Symplekin and xGLD-2 are required for CPEB-mediated cytoplasmic polyadenylation. Cell *119*, 641–651.

Bilger, A., Fox, C.A., Wahle, E., and Wickens, M. (1994). Nuclear polyadenylation factors recognize cytoplasmic polyadenylation elements. Genes Dev. *8*, 1106–1116.

Charlesworth, A., Welk, J., and MacNicol, A.M. (2000). The temporal control of Wee1 mRNA translation during Xenopus oocyte maturation is regulated by cytoplasmic polyadenylation elements within the 3′-untranslated region. Dev. Biol. *227*, 706–719.

Charlesworth, A., Cox, L.L., and MacNicol, A.M. (2004). Cytoplasmic polyadenylation element (CPE)- and CPE-binding protein (CPEB)-independent mechanisms regulate early class maternal mRNA translational activation in Xenopus oocytes. J. Biol. Chem. *279*, 17650–17659.

Charlesworth, A., Wilczynska, A., Thampi, P., Cox, L.L., and MacNicol, A.M. (2006). Musashi regulates the temporal order of mRNA translation during Xenopus oocyte maturation. EMBO J. *25*, 2792–2801.

de Moor, C.H., and Richter, J.D. (1997). The Mos pathway regulates cytoplasmic polyadenylation in Xenopus oocytes. Mol. Cell. Biol. *17*, 6419–6426.

de Moor, C.H., and Richter, J.D. (1999). Cytoplasmic polyadenylation elements mediate masking and unmasking of cyclin B1 mRNA. EMBO J. *18*, 2294–2303.

Dickson, K.S., Bilger, A., Ballantyne, S., and Wickens, M.P. (1999). The cleavage and polyadenylation specificity factor in Xenopus laevis oocytes is a cytoplasmic factor involved in regulated polyadenylation. Mol. Cell. Biol. *19*, 5707–5717.

Fox, C.A., Sheets, M.D., and Wickens, M.P. (1989). Poly(A) addition during maturation of frog oocytes: distinct nuclear and cytoplasmic activities and regulation by the sequence UUUUUAU. Genes Dev. *3*, 2151–2162.

Hake, L.E., and Richter, J.D. (1994). CPEB is a specificity factor that mediates cytoplasmic polyadenylation during Xenopus oocyte maturation. Cell *79*, 617–627.

Hochegger, H., Klotzbucher, A., Kirk, J., Howell, M., le Guellec, K., Fletcher, K., Duncan, T., Sohail, M., and Hunt, T. (2001). New B-type cyclin synthesis is required between meiosis I and II during Xenopus oocyte maturation. Development *128*, 3795–3807.

Kim, J.H., and Richter, J.D. (2006). Opposing polymerase-deadenylase activities regulate cytoplasmic polyadenylation. Mol. Cell *24*, 173–183.

Klein, D.J., Schmeing, T.M., Moore, P.B., and Steitz, T.A. (2001). The kink-turn: a new RNA secondary structure motif. EMBO J. *20*, 4214–4221.

Mendez, R., and Richter, J.D. (2001). Translational control by CPEB: a means to the end. Nat. Rev. Mol. Cell Biol. *2*, 521–529.

Mendez, R., Hake, L.E., Andresson, T., Littlepage, L.E., Ruderman, J.V., and Richter, J.D. (2000a). Phosphorylation of CPE binding factor by Eg2 regulates translation of c-mos mRNA. Nature *404*, 302–307.

Mendez, R., Murthy, K.G., Ryan, K., Manley, J.L., and Richter, J.D. (2000b). Phosphorylation of CPEB by Eg2 mediates the recruitment of CPSF into an active cytoplasmic polyadenylation complex. Mol. Cell *6*, 1253–1259.

Mendez, R., Barnard, D., and Richter, J.D. (2002). Differential mRNA translation and meiotic progression require Cdc2-mediated CPEB destruction. EMBO J. *21*, 1833–1844.

Murray, M.T., Schiller, D.L., and Franke, W.W. (1992). Sequence analysis of cytoplasmic mRNA-binding proteins of Xenopus oocytes identifies a family of RNA-binding proteins. Proc. Natl. Acad. Sci. USA *89*, 11–15.

Nakahata, S., Katsu, Y., Mita, K., Inoue, K., Nagahama, Y., and Yamashita, M. (2001). Biochemical identification of Xenopus Pumilio as a sequence-specific cyclin B1 mRNA-binding protein that physically interacts with a Nanos homolog, Xcat-2, and a cytoplasmic polyadenylation element-binding protein. J. Biol. Chem. *276*, 20945–20953.

Nakahata, S., Kotani, T., Mita, K., Kawasaki, T., Katsu, Y., Nagahama, Y., and Yamashita, M. (2003). Involvement of Xenopus Pumilio in the translational regulation that is specific to cyclin B1 mRNA during oocyte maturation. Mech. Dev. *120*, 865–880.

Okano, H., Imai, T., and Okabe, M. (2002). Musashi: a translational regulator of cell fate. J. Cell Sci. *115*, 1355–1359.

Pique, M., Lopez, J.M., and Mendez, R. (2006). Cytoplasmic mRNA polyadenylation and translation assays. In Xenopus Protocols:cell biology and signal transduction, X. Johné Liu, ed. (Totowa, New Jersey: Humana Press Inc), pp. 183–198.

Reverte, C.G., Ahearn, M.D., and Hake, L.E. (2001). CPEB degradation during Xenopus oocyte maturation requires a PEST domain and the 26S proteasome. Dev. Biol. *231*, 447–458.

Richter, J.D. (2007). CPEB: a life in translation. Trends Biochem. Sci. *32*, 279–285.

Rouhana, L., Wang, L., Buter, N., Kwak, J.E., Schiltz, C.A., Gonzalez, T., Kelley, A.E., Landry, C.F., and Wickens, M. (2005). Vertebrate GLD2 poly(A) polymerases in the germline and the brain. RNA *11*, 1117–1130.

Rouhana, L., and Wickens, M. (2007). Autoregulation of GLD-2 cytoplasmic poly(A) polymerase. RNA *13*, 188–199.

Sagata, N., Oskarsson, M., Copeland, T., Brumbaugh, J., and Vande Woude, G.F. (1988). Function of c-mos proto-oncogene product in meiotic maturation in Xenopus oocytes. Nature *335*, 519–525.

Sheets, M.D., Fox, C.A., Hunt, T., Vande Woude, G., and Wickens, M. (1994). The 3′-untranslated regions of c-mos and cyclin mRNAs stimulate translation by regulating cytoplasmic polyadenylation. Genes Dev. *8*, 926–938.

Stebbins-Boaz, B., Hake, L.E., and Richter, J.D. (1996). CPEB controls the cytoplasmic polyadenylation of cyclin, Cdk2 and c-mos mRNAs and is necessary for oocyte maturation in Xenopus. EMBO J. *15*, 2582–2592.

Stebbins-Boaz, B., Cao, Q., de Moor, C.H., Mendez, R., and Richter, J.D. (1999). Maskin is a CPEB-associated factor that transiently interacts with eIF-4E. Mol. Cell *4*, 1017–1027.